JACS
JOURNAL OF THE AMERICAN CHEMICAL SOCIETY
Article
pubs.acs.org/JACS

Isolation and Structure Elucidation of Ovatoxin-a, the Major Toxin Produced by *Ostreopsis ovata*

Patrizia Ciminiello, Carmela Dell'Aversano, Emma Dello Iacovo, Ernesto Fattorusso, Martino Forino,* Laura Grauso, and Luciana Tartaglione

Dipartimento di Chimica delle Sostanze Naturali, University of Napoli "Federico II", Via D. Montesano 49, 80131 Napoli, Italy

Franca Guerrini, Laura Pezzolesi, and Rossella Pistocchi

Centro Interdipartimentale di Ricerca per le Scienze Ambientali, Via S. Alberto 163, 48100 Ravenna, Italy

Silvana Vanucci

Dipartimento di Biologia Animale ed Ecologia Marina, Università di Messina, Viale Ferdinando d'Alcontres 31, 98166 S. Agata, Messina, Italy

Supporting Information

ABSTRACT: Since 2005, the benthic dinoflagellate *Ostreopsis* cf. *ovata* has bloomed across the Mediterranean basin, provoking serious toxic outbreaks. LC/MS studies have identified a number of palytoxin-like compounds, termed ovatoxins, along with trace amounts of putative palytoxin as the causative agents of the *O.* cf. *ovata*-related human sufferings. So far, any risk assessment for ovatoxins as well as establishment of their allowance levels in seafood has been prevented by the lack of pure toxins. The present paper reports on the isolation, NMR-based structural determination, and preliminary mouse lethality evaluation of ovatoxin-a, the major toxic compound contained in *O.* cf. *ovata* extracts. Availability of pure ovatoxin-a will open the double prospect of fully evaluating its toxicity and preparing reference standards to be employed in LC/MS quantitative analyses. Elucidation of ovatoxin-a's complex structure will ultimately herald the understanding of the molecular bases of ovatoxins bioactivity.

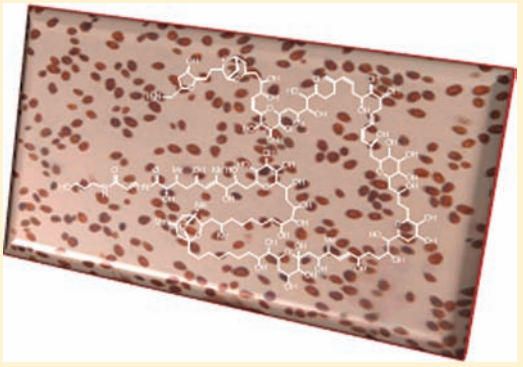

INTRODUCTION

In the summer of 2005, abnormal concentrations of *Ostreopsis* cf. *ovata* caused grave human intoxications along the northern Tyrrhenian coast of Italy.[1] Ever since, this tropical dinoflagellate has bloomed every summer across the Mediterranean Sea, affecting marine environment, public health, and maritime economy as well. Our research group, prompted by the toxic events of 2005, has started a scientific study aimed at investigating the toxin content of samples of Mediterranean *O.* cf. *ovata*. On account of the recurring blooms of the above alga, in collaboration with governmental agencies in charge of safeguarding public health, we have been involved in *O.* cf. *ovata* monitoring programs along the Italian coastline. Liquid chromatography−mass spectrometry (LC/MS)-based analyses have led us to identify—in both field and cultured samples of *O.* cf. *ovata* —initially a putative palytoxin,[1] and successively a number of much more abundant palytoxin-like compounds we named ovatoxins (OVTXs).[2] Among all of the OVTXs so far detected, namely, OVTX-a, -b, -c, -d, and -e, OVTX-a is by far the major toxin contained in *O.* cf. *ovata* extracts.[3] Unfortunately, in the case of OVTXs, as often happens in the field of marine biotoxins, scientific research has been significantly limited by scarce availability of pure compounds. So, despite the serious health-related concerns OVTXs raise across the EU, the European Food Safety Authority (EFSA) has not been able to assess the real risks they pose to humans and, consequently, to set the allowance levels of such toxins in seafood, because of a substantial lack of referenced material.[4]

The present paper reports on the isolation, NMR-driven structural elucidation, and preliminary mouse lethality assessment of OVTX-a. The availability of pure OVTX-a will finally allow studies on its toxicity to start and provide reference standards for accurate quantitative LC/MS analyses. In addition, identification of OVTX-a's complex chemical architecture will ultimately offer the prospect of understanding the molecular bases of its bioactivity.

Received: November 16, 2011
Published: December 27, 2011

dx.doi.org/10.1021/ja210784u | *J. Am. Chem.Soc.* 2012, 134, 1869−1875

EXPERIMENTAL SECTION

1. *O.* cf. *ovata* Cultures. *O.* cf. *ovata* strains isolated by the capillary pipet method[5] from water samples collected along the Adriatic and Tyrrhenian coasts of Italy in 2006−2008 were cultured. Adriatic strains were OOAN0601 (from Numana, Marche region, isolated in 2006), OOAN0709 (from Numana, Marche region, isolated in 2007), OOAN0816 (from Numana, Marche region, isolated in 2008), and OOAB0801 (from Bari, Puglia region, isolated in 2008); the Tyrrhenian strain was OOTL0707 (from Latina, Lazio region, isolated in 2007). Cultures were established at a salinity of 36 and temperature of 20 °C, in a thermostatic room under a 16:8 h light:dark cycle from a cool white lamp, maintaining light irradiance at 100−110 μmol m^{-2} s^{-1}. In order to evaluate the toxin content of *O.* cf. *ovata* strains, cultures were prepared adding macronutrients at a 5-fold diluted *f*/2 concentrations with selenium.[6]

For each isolate, two 400 mL culturing flasks were set up for the evaluation of toxin content, and culture collections were carried out during the late stationary growth phases (day 25) by gravity filtration through GF/F Whatman (0.7 μm) filters. Only cell pellets were provided for chemical analysis, considering that the recovery of OVTXs released into the growth media (45%) is remarkably lower than that obtained if OVTXs are extracted from pellets (98%).[7]

2. Extraction. To each cell pellet sample was added 8 mL of a methanol/water (1:1, v/v) solution and the sample was sonicated for 30 min in pulse mode, while being cooled in an ice bath. The mixture was centrifuged at 3000*g* for 30 min, the supernatant was decanted, and the pellet was washed twice with 8 mL of methanol/water (1:1, v/v). The extracts were combined and the volume was adjusted to 24 mL with extracting solvent. The obtained mixture was analyzed directly by HR LC/MS (5 μL injected). The recovery percentage of the above extraction procedure for the pellet was estimated to be 98%.[2]

3. Data Analysis. Differences in toxin profile among the algal extracts were tested by using the multivariate analysis-of-variance (ANOVA) test, using Statistica (StatSoft, Tulsa, OK) software. Whenever a significant difference for the main effect was observed ($P < 0.05$), a Newman−Keuls test was also performed.

4. Isolation. *O.* cf. *ovata* cells from over 80 L of OOAN0816 strain cultures were collected by filtration, suspended in MeOH:H_2O:AcOH (50:50:0.1), sonicated, and finally centrifuged. The resulting pellet was subjected to the same procedure as above two more times. Once combined, the three obtained extracts were partitioned with CH_2Cl_2. The aqueous layer containing OVTXs was evaporated in vacuo at 28 °C, loaded onto a 360-g Combiflash C-18 column connected to a Teledyne Isco Combi*Flash* R_f flash chromatography system, and eluted with H_2O:PrOH, the ratio of which changed from 60:40 to 10:90 in 50 min. A 75-mL fraction containing OVTXs was collected after 13 min. This fraction was concentrated and further separated on a Gemini 10 μm HPLC column (Phenomenex, Torrance, CA) connected to a SpectraSYSTEM HPLC model P2000, by gradient elution with changing ratios of H_2O:CH_3CN:AcOH from 80:20:01 to 0:100:0.1 in 30 min. The final purification of OVTX-a was achieved on a Kinetex 2.6 μm HPLC column (Phenomenex, Torrance, CA) connected to an Agilent HPLC model 1100 (Palo Alto, CA) coupled to a linear ion trap LTQ Orbitrap XL hybrid Fourier transform MS (FTMS) equipped with an ESI ION MAX source (Thermo-Fisher, San Josè, CA). This last purification was carried out by using a 20-min gradient with the same mobile phases as above.

5. NMR Experiments. NMR spectra were measured on a Varian Unity Inova 700 spectrometer equipped with a 13C Enhanced HCN Cold Probe. Shigemi 5 mm NMR tubes and CD_3OD as an internal standard (δ_H 3.31 and δ_C 49.0) were used. Standard Varian pulse sequences were employed for the respective classes of spectra; solvent signal suppression by presaturation was used when required. All NMR data reported in the text were derived from 2D $^1H-^1H$ COSY, z-filtered TOCSY, ROESY, phase-sensitive HMBC, HSQC, and HSQCTOCSY spectra.

6. Mouse Lethality Measurement. Mouse lethality of OVTX-a was assayed in female mice (20 ± 0.5 g) by intraperitoneal injection of toxin solutions with 1% Tween 60. Injection volume was 500 μL. OVTX-a was tested at a dose level of 7.0 μg/kg. Three mice were used and kept under observation for 30 min.

RESULTS AND DISCUSSION

1. Analysis of Mediterranean *O.* cf. *ovata* Strains. Selection of the Strain To Be Cultivated. Since different strains of *O.* cf. *ovata* feature different toxin profiles,[7] we decided to analyze the toxin content of five *O.* cf. *ovata* strains recently collected from the Mediterranean Sea. The aim of this analysis was selecting the most suitable strain to be large-scale cultivated for isolation of OVTX-a. LC/MS investigation performed on four strains (i.e., OOTL0707, OOAB0801, OOAN0709, and OOAN0601) indicated that all of them possessed roughly the same OVTXs content as that detected in most of the *O.* cf. *ovata* strains so far studied.[7] In more detail, OVTX-a turned out to be by far the major component of the toxin profile (53−57% of the total toxin content; Posthoc SNK test, $P < 0.001$), followed by OVTX-b (24−26%), OVTX-d/-e (12−14%), OVTX-c (4−5%), and putative palytoxin (1−4%) (Figure 1). These percentages were evaluated by using

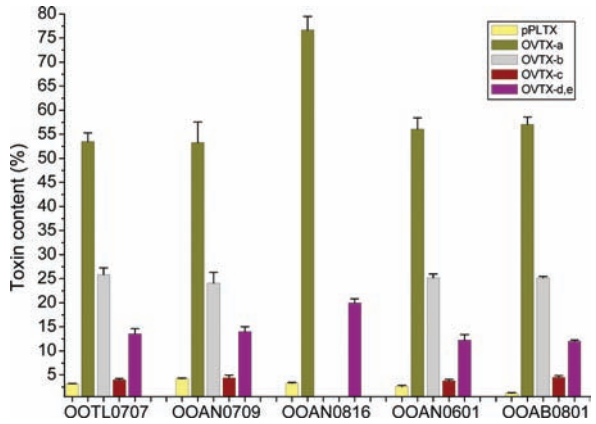

Figure 1. Individual toxin contents of putative palytoxin, OVTX-a, -b, -c, -d, and -e of several Adriatic and Tyrrhenian *O.* cf. *ovata* strains in the stationary phase. HR LC/MS measurements were carried out for cell pellet extracts and expressed as toxin percentage (%).

palytoxin reference standard and assuming that OVTXs have the same molar response as palytoxin itself. Conversely, the strain termed OOAN0816, isolated from the Adriatic Sea nearby Ancona, Italy, featured a different toxin profile. In fact, in the toxic extract of this strain OVTX-a accounted for about 77% of the toxin content, OVTX-d/-e for 20%, and putative palytoxin was at around 3%. Interestingly, OVTX-b and -c were totally missing (Figure 1). This was further confirmed by subsequent analyses of algal extracts from the same strain grown under different conditions. Once again the existing differences among *O.* cf. *ovata* strains, in terms of toxin production, were proven, while for the first time the absence of two out of the six commonly occurring OVTXs in one *O.* cf. *ovata* strain was ascertained.

Obtaining OVTXs in pure form is challenging, in that they account only for a small percentage in comparison with other much more abundant cellular metabolites. Additionally, differing from each other only by little structural details, the chromatographic behavior of all of OVTXs is nearly identical, with OVTX-b and -c eluting very close to OVTX-a. Thus, the finding that OVTX-b and -c were not produced by OOAN0816

was decisive for selecting this as the best strain to be large-scale cultured.

2. Isolation of Ovatoxin-a. The aqueous extract containing OVTXs deriving from over 80 L of OOAN0816 strain cultures was first purified on a 360-g Combiflash C-18 column and then on a Gemini 10 μm HPLC column. Final purification of OVTX-a was achieved on a Kinetex 2.6 μm HPLC column (see Experimental Section). The presence of OVTX-a in each eluate was checked by high-resolution LC/MS analysis in full MS mode (positive ions). Eventually, we obtained 700 μg of OVTX-a.

3. Structural Elucidation of Ovatoxin-a. High-resolution full MS spectrum of OVTX-a—acquired on a hybrid linear ion trap FTMS instrument—generated a monocharged ion $[M + H]^+$ (monoisotopic ion at m/z 2647.4979) corresponding to the molecular formula $C_{129}H_{223}N_3O_{52}$ (Δ = −3.918 ppm).[3]

The chemical structure of OVTX-a was determined through thorough interpretation of 1D and 2D NMR experiments (^{1}H NMR, ^{1}H−^{1}H COSY, z-TOCSY, ROESY, HSQC, HMBC, and HSQCTOCSY) run on a 700 MHz instrument equipped with a cryoprobe. Due to the relatively small amount of pure compound, we could not afford any reliable ^{13}C spectrum. As a consequence, we resorted to HSQC and HMBC experiments for identifying OVTX-a's protonated and quaternary carbons, respectively.

A comprehensive analysis of OVTX-a's spin systems, mainly obtained by interpreting ^{1}H−^{1}H COSY and z-TOCSY, highlighted broad analogies between OVTX-a and both palytoxin and 42-hydroxypalytoxin,[8] recently characterized by our group (Figure 2). It followed that we could adopt NMR

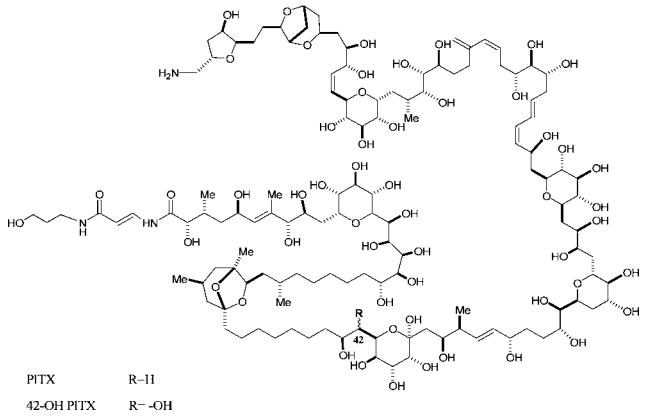

Figure 2. Stereostructure of palytoxin and 42-hydroxypalytoxin.

data reported for palytoxin[9] and 42-hydroxypalytoxin as a guide in our NMR-driven structural elucidation of OVTX-a (Table 1). More specifically, the NMR data relative to the part of OVTX-a's structure stretching out from position 8′ through 7 as well as those of the regions extending from position 29 to 32 and from position 73 up to the terminal position 115 (Figure 3) appeared nearly superimposable with the reference NMR data of both palytoxin and 42-hydroxypalytoxin. Hence, we could confidently conclude that OVTX-a shared not only the same planar structure but also the same stereochemistry as palytoxin and 42-hydroxypalytoxin in the above-mentioned segments. On the contrary, apart from the part structure comprised between positions 29 and 32, the central region of OVTX-a from position 8 to 72 showed remarkable differences in comparison to palytoxin and 42-hydroxypalytoxin. Accordingly, assignment of the chemical structure of this region was carried out de novo on the basis of experimental evidence derived from NMR experiments.

Here below, we detail the key steps of our NMR-based structural investigation that led us to fully elucidate the chemical architecture of OVTX-a. Our analysis was focused on the following three spin systems contained in the central region of OVTX-a (Figure 3): A spin system (C8−C28), B spin system (C34−C46), and C spin system (C48−C84).

All of the obtained NMR spectra relative to OVTX-a are reported in the Supporting Information (S1−S7) alongside some enlargements of all those NMR experiments that proved crucial for the structural analysis of our molecule (S8−S20).

3.1. Elucidation of the A Spin System (Figure 4a). Our study started by identifying C8 (δ 80.90) thanks to its key HMBC correlation with the methyl at position 7 (δ 1.74) (Supporting Information, S8). Then, C8 was connected to its proton (δ 3.91) by means of the HSQC spectrum. Unfortunately, the NMR signal of H9 (δ 3.92) was basically overlapping with that of H8. However, we could define the proton sequence stretching from position 8 through 11 on the basis of the following NMR evidence: (i) HMBC correlations between H8 and C9 (δ 70.68) and between H10b (δ 2.11) and C8 (Supporting Information, S9a) and (ii) H^1−H^1 COSY cross-peaks between H9 and $H_2$10 (δ 1.80, 2.11) as well as between $H_2$10 and H11 (δ 4.11). Such a connectivity was definitively confirmed by the z-TOCSY experiment (Supporting Information, S9b).

Moving on along the carbon chain of the molecule, we came across a very congested region of the NMR spectra, namely, the C12−C19 segment, characterized by strong overlapping of the chemical shifts of protons and carbons (Table 1). We succeeded in disentangling this intricate segment through a careful analysis of H^1−H^1 COSY and z-TOCSY supported by a parallel analysis of HSQC and HMBC correlations (the latter are reported in Figure 4a) (see also the Supporting Information, S10 and S11).

This complex step of our structural investigation, leading as far as position 19, allowed us to pinpoint the first structural modification between OVTX-a and both palytoxin and 42-hydroxypalytoxin. In fact, all of the NMR data relative to this region were consistent with the occurrence of a methylene at position 17 (δ_H 1.33, 1.52; δ_C 45.60) instead of a hydroxyl group. At this point of our structure analysis, identification of H20 (3.88), the chemical shift of which was basically overlapping with that of H18 (3.87), was feasible thanks to clear HMBC correlations between H21b and both C20 (68.10) and C19 (69.90) and between $H_2$22 (1.40) and C20 (Supporting Information, S12).

In parallel, analysis of H^1−H^1 COSY, z-TOCSY, HSQC, HMBC, and HSQCTOCSY was decisive for elucidating the remaining part of the A spin system up to position 28 (δ_H 3.97, δ_C 79.94), which turned out to parallel that of both palytoxin and 42-hydroxypalytoxin.

Advancing on OVTX-a's carbon chain, we encountered the C29−C32 spin system that, as previously reported, appeared superimposable with the relevant spin system of both palytoxin and 42-hydroxypalytoxin. Thus our NMR investigation shifted toward identification of the B spin system.

3.2. Elucidation of the B Spin System (Figure 4b). The acetal carbon at position 33 (δ 109.00) was identified thanks to HMBC correlations between this carbon and both H28 and $H_2$34 (δ_H 1.60, δ_C 39.32) (Supporting Information, S13). The

dx.doi.org/10.1021/ja210784u | J. Am. Chem.Soc. 2012, 134, 1869−1875

Table 1. ^{1}H and ^{13}C NMR Chemical Shift Data of Palytoxin,[9] OVTX-a, and 42-Hydroxypalytoxin

	palytoxin		OVTX-a		42-OH-palytoxin			palytoxin		OVTX-a		42-OH-palytoxin	
no.	^{13}C	^{1}H	^{13}C	^{1}H	^{13}C	^{1}H	no.	^{13}C	^{1}H	^{13}C	^{1}H	^{13}C	^{1}H
1	175.92	–	175.93	–	175.76	–	60	70.18	3.85	68.82	3.82	70.21	3.85
2	75.70	4.09	75.12	4.09	75.68	4.08	61	76.57	3.15	75.70	3.14	76.57	3.15
3	34.73	2.17	34.54	2.14	34.89	2.18	62	73.11	3.74	76.75	3.42	73.15	3.75
3-Me	13.99	0.88	13.94	0.86	14.13	0.88	63	36.77	1.70	29.55	1.52	36.89	1.70
									1.96		2.03		1.96
4	41.73	1.40	41.31	1.39	41.82	1.40	64	71.77	3.68	35.20	1.50	71.88	3.68
		1.77		1.79		1.76					1.71		
5	66.62	4.50	66.40	4.51	66.67	4.50	65	72.20	3.76	73.57	3.86	72.27	3.76
6	131.85	5.49	131.51	5.49	131.82	5.49	66	37.01	1.53	40.68	1.55	37.16	1.54
									2.04		1.93		2.04
7	138.28	–	138.31	–	138.26	–	67	77.22	3.44	76.72	3.45	77.16	3.44
7-Me	13.17	1.72	13.22	1.74	13.34	1.72	68	76.04	3.12	75.57	3.10	76.04	3.12
8	80.91	3.92	80.90	3.91	80.97	3.92	69	79.74	3.36	79.31	3.35	79.81	3.36
9	72.34	3.81	70.68	3.92	72.30	3.82	70	75.85	3.09	75.49	3.09	75.95	3.09
10	29.23	2.12	27.95	1.80	29.36	2.13	71	77.08	3.44	76.70	3.41	77.08	3.43
				2.11									
11	76.19	4.18	77.15	4.11	76.26	4.17	72	41.51	1.43	41.11	1.42	41.69	1.40
									2.04		2.03		2.04
12	73.88	3.64	74.26	3.65	73.68	3.65	73	64.99	4.84	64.86	4.82	65.03	4.84
13	75.17	3.54	74.55	3.57	75.18	3.55	74	133.47	5.37	133.10	5.37	133.45	5.37
14	71.68	3.60	71.32	3.58	71.82	3.59	75	130.04	6.00	129.85	5.99	139.99	6.00
15	72.91	3.62	74.55	3.58	72.91	3.62	76	128.87	6.46	128.44	6.43	128.87	6.46
16	71.28	4.03	74.34	4.04	71.35	4.03	77	133.88	5.78	133.58	5.78	133.95	5.78
17	71.68	4.04	45.60	1.33	71.64	4.04	78	38.64	2.42	38.54	2.40	38.81	2.41
				1.52									
18	73.27	3.54	68.43	3.87	73.29	3.54	79	71.20	3.93	72.60	3.93	71.22	3.93
19	71.35	3.79	69.90	4.05	71.30	3.79	80	76.29	3.27	76.03	3.26	76.34	3.26
20	71.11	3.87	68.10	3.88	71.19	3.88	81	73.04	3.63	72.74	3.69	73.10	3.71
21	27.38	1.39	29.00	1.32	27.70	1.37	82	34.35	2.39	34.00	2.37	34.56	2.39
		1.48		1.63		1.49			2.75		2.75		2.76
22	26.93	1.35	27.11	1.40	27.40	1.35	83	130.18	5.69	129.91	5.68	130.26	5.69
		1.47				1.48							
23	35.03	1.55	34.82	1.23	35.16	1.55	84	132.64	5.95	132.27	5.94	132.67	5.95
		1.64		1.58		1.64							
24	28.44	1.36	30.43	1.22	28.70	1.36	85	146.73	–	146.33	–	146.63	–
				1.47									
25	39.72	1.26	40.12	1.14	39.89	1.26	85′	114.86	4.94	114.74	4.92	114.92	4.94
				1.30					5.07		5.05		5.07
26	29.70	1.67	30.01	1.61	29.83	1.68	86	34.30	2.25	34.01	2.23	34.56	2.25
									2.34		2.32		2.34
26-Me	19.30	0.92	21.41	0.92	19.50	0.92	87	33.13	1.59	32.77	1.59	33.17	1.58
									1.72		1.73		1.72
27	40.78	0.91	39.35	0.78	40.77	0.90	88	74.19	3.71	73.92	3.70	74.29	3.71
		1.47		1.60		1.48							
28	80.17	3.97	79.94	3.97	80.22	3.97	89	74.02	3.50	73.56	3.50	74.02	3.50
29	82.31	–	82.20	–	82.27	–	90	77.82	3.35	77.59	3.35	77.93	3.35
29-Me	21.01	1.18	20.70	1.18	21.15	1.18	91	33.00	1.89	32.71	1.88	33.16	1.89
30	45.74	1.14	45.44	1.14	45.92	1.15	91-Me	15.65	0.91	15.38	0.90	15.78	0.91
		1.70		1.71		1.70							
31	25.55	2.04	25.25	2.06	25.77	2.05	92	27.86	1.30	27.61	1.28	27.97	1.30
									2.21		2.20		2.22
31-Me	21.89	0.91	21.61	0.91	22.00	0.92	93	74.83	4.03	74.51	4.03	74.90	4.03
32	43.74	1.09	44.10	1.08	43.94	1.09	94	73.04	3.65	72.58	3.64	73.13	3.64
		1.67		1.65		1.68							
33	109.23	–	109.00	–	109.24	–	95	74.73	3.61	74.42	3.61	74.74	3.61
34	38.64	1.60	39.32	1.60	38.69	1.60	96	76.01	3.15	75.71	3.16	76.01	3.15
35	23.98	1.41	24.11	1.43	24.23	1.43	97	69.71	4.32	69.35	4.31	69.74	4.32
36	30.98	1.31	30.50	1.27	30.84	1.29	98	132.43	5.55	132.11	5.54	132.41	5.54
37	30.93	1.31	30.50	1.27	30.84	1.29	99	135.28	5.71	135.08	5.70	135.31	5.70

dx.doi.org/10.1021/ja210784u | J. Am. Chem.Soc. 2012, 134, 1869–1875

Table 1. continued

	palytoxin		OVTX-a		42-OH-palytoxin			palytoxin		OVTX-a		42-OH-palytoxin	
no.	^{13}C	^{1}H	^{13}C	^{1}H	^{13}C	^{1}H	no.	^{13}C	^{1}H	^{13}C	^{1}H	^{13}C	^{1}H
38	30.81	1.31	31.71	1.35	30.84	1.29	100	71.90	4.36	71.64	4.36	71.94	4.37
39	31.29	1.36	28.50	1.27	31.21	1.35	101	71.77	3.68	71.50	3.67	71.88	3.68
				1.68									
40	39.20	1.48	34.81	1.20	38.69	1.58	102	40.21	1.58	39.79	1.57	40.33	1.59
				1.87									
41	69.26	3.80	71.95	3.66	71.92	3.65	103	68.39	4.22	68.12	4.21	68.38	4.22
42	39.37	1.44	77.73	3.05	77.34	3.70	104	40.53	1.38	40.21	1.37	40.72	1.38
		1.86							1.74		1.73		1.74
43	64.86	4.39	63.11	4.63	66.10	4.32	105	76.14	4.51	75.91	4.51	76.21	4.51
44	73.88	3.65	34.49	1.63	74.08	3.91	106	36.83	1.78	36.48	1.76	36.96	1.79
				2.01					1.84		1.85		1.84
45	74.28	3.95	69.81	4.28	74.28	3.91	107	79.62	4.21	79.40	4.21	79.61	4.21
46	68.25	3.67	71.52	3.41	67.75	3.78	108	82.74	4.35	82.51	4.35	82.80	4.36
47	101.24	–	101.16	–	101.59	–	109	26.59	1.67	26.33	1.64	26.83	1.66
									1.78		1.78		1.78
48	41.95	1.83	40.34	1.74	41.92	1.77	110	32.30	1.47	32.11	1.48	32.47	1.48
49	72.40	3.94	72.49	3.82	72.45	3.92	111	83.81	3.89	83.64	3.89	83.87	3.89
50	44.07	2.26	43.55	2.29	44.41	2.25	112	73.27	4.27	72.92	4.27	73.31	4.27
50-Me	16.58	1.03	16.82	1.05	16.72	1.03	113	39.78	1.86	39.46	1.87	39.89	1.86
									2.10		2.11		2.11
51	134.46	5.62	134.51	5.62	134.59	5.64	114	75.31	4.36	74.46	4.38	75.14	4.37
52	134.74	5.51	134.14	5.47	134.69	5.50	115	45.13	2.87	44.49	2.91	45.13	2.90
									2.99		3.05		3.03
53	74.06	4.05	73.92	4.01	74.06	4.06	2′	134.82	7.79	134.81	7.80	134.76	7.80
54	34.93	1.61	34.82	1.57	35.09	1.61	3′	106.82	5.95	106.82	5.94	106.79	5.95
		1.77		1.76		1.78							
55	27.79	1.46	27.18	1.43	27.89	1.46	4′	169.66	–	169.39	–	169.57	–
		1.69		1.63		1.69							
56	73.11	3.74	72.75	3.66	73.15	3.75	6′	37.42	3.33	37.53	3.34	37.51	3.33
57	72.81	3.85	71.67	3.87	72.86	3.86	7′	33.28	1.74	33.19	1.73	33.46	1.74
58	74.19	3.87	70.91	3.86	74.11	3.87	8′	60.40	3.60	60.40	3.59	60.60	3.59
59	33.05	1.66	32.72	1.65	33.16	1.66							
		2.27		2.27		2.26							

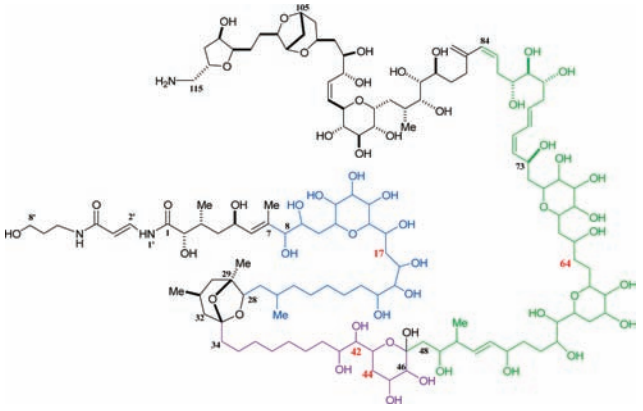

Figure 3. Chemical structure of OVTX-a. Positions where structural differences between OVTX-a and palytoxin occur are indicated in red. The A spin system is colored in blue, the B spin system in purple, and the C spin system in green. The stereochemistry reported in the figure has been assumed to be the same as that of palytoxin on the basis of a substantial overlapping of both protons and carbons chemical shifts of OVTX-a with the corresponding ones of palytoxin itself.

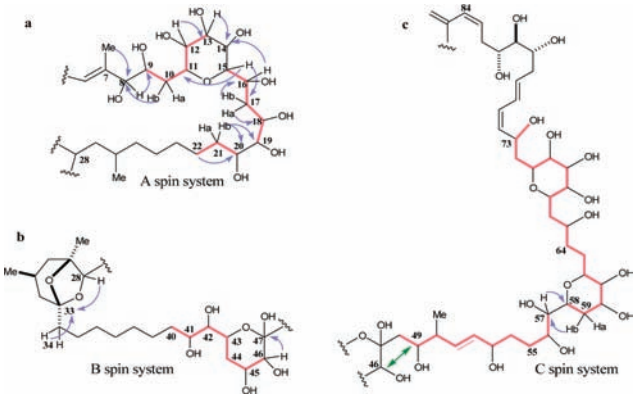

Figure 4. (a) The structural segment of (a) the A spin system of OVTX-a, (b) the B spin system of OVTX-a, (c) the C spin system of OVTX-a. In pink bold lines are depicted carbons linking protons whose connectivity was identified through ^{1}H−^{1}H COSY. Blue arrows indicate key HMBC correlations; the green arrow indicates a ROE correlation.

identified methylene at position 34 constituted the first member of a 7-methylene aliphatic chain of the B spin system that was wholly defined through H^{1}−H^{1} COSY, z-TOCSY, HSQC, and HMBC. Such an aliphatic chain ended up at position 40 (δ_H 1.20, 1.87; δ_C 34.81) that was in turn coupled to a hydroxy methine functionality (δ_H 3.66, δ_C 71.95) at position 41. H^{1}−H^{1} COSY and z-TOCSY led to identification

dx.doi.org/10.1021/ja210784u | J. Am. Chem.Soc. 2012, 134, 1869−1875

of the C41−C46 segment, of which the chemical shift values of the protons and carbons were fortunately not overlapping with each other (Supporting Information, S14). In this terminal segment of the B spin system, further structural modifications in the face of palytoxin were detected. In more detail, like 42-hydroxypalytoxin, OVTX-a featured a hydroxyl group at C42 (δ_H 3.05, δ_C 77.73), but unlike palytoxin and 42-hydroxypalytoxin, it presented a methylene (δ_H 1.63, 2.01; δ_C 34.49) at position 44 instead of a hydroxy methine functionality.

3.3. Elucidation of the C Spin System (Figure 4c). ROE between H46 and H49 (δ 3.82) was crucial for linking the B spin system to the C one (Supporting Information, S15a). Indeed, these two systems appeared connected to each other through a hemiacetal functionality at position 47 (δ 101.16) individuated on the basis of HMBC correlations of C47 with H46 (δ 3.41) (Supporting Information, S15b). Proceeding from $H_2$48 (δ 1.74), identified in the H^1−H^1 COSY thanks to its vicinal coupling with H49, we could define the C spin system up to position 55, benefiting from a substantial correspondence of NMR data of OVTX-a with those of palytoxin and 42-hydroxypalytoxin. From position 56 onward more significant differences in chemical shifts between OVTX-a and both palytoxin and 42-hydroxypalytoxin arose. However, connectivity from position 55 through 57 (δ_H 3.87, δ_C 71.67) was established on the basis of H^1−H^1 COSY, z-TOCSY, and HSQC (Supporting Information, S16). Unfortunately, H58 (δ 3.86) resonated too close to H57 for us to detect a cross peak in the COSY experiment. Nonetheless, HMBC correlations between H59b (δ 2.27) and C57 as well as between H57 and C58 (δ 70.91) (Supporting Information, S17a and S17b) along with clear vicinal proton−proton coupling between $H_2$59 (δ 1.65, 2.27) and H58 helped us to elucidate the proton connectivity up to position 59. Detailed NMR-based analysis of COSY, z-TOCSY, and HSQC experiments allowed identification of the planar structure of OVTX-a up to position 73 (δ_H 4.82, δ_C 64.86) (Supporting Information, S18−S20). The last structural divergence between OVTX-a and both palytoxin and 42-hydroxypalytoxin emerged at position 64 (δ_H 1.50, 1.71; δ_C 35.20), where the lack of a hydroxyl group was detected. Once we assessed the connectivity between positions 73 and 74 (δ_H 5.37, δ_C 133.10), the remaining part of the molecule was easily individuated as NMR data of OVTX-a started aligning again with those of palytoxin and 42-hydroxypalytoxin (Figure 4c).

Eventually, the structure of OVTX-a was identified as shown in Figure 3.

4. Mouse Lethality Assessment. Mouse lethality assessment of OVTX-a was tested at a dose level of 7.0 μg/kg. One to 3 min after injection, mice started wriggling and all died within 30 min with paralyzed limbs. These preliminary studies on OVTX-a's toxicity led us to conclude that the toxin mouse lethality lies below 7.0 μg/kg.

CONCLUSIONS

The complex structure of OVTX-a, encompassing 129 carbons and 223 protons, was reflected in heavily congested NMR spectra, whose interpretation was undoubtedly challenging. However, the structural analysis of OVTX-a was partly eased by comparison of its NMR data with those of palytoxin reported in literature as well as with those of 42-hydroxypalytoxin characterized by us in 2009.

It is noteworthy that the NMR-derived structure of OVTX-a appeared totally consistent with the structural evidence obtained for this toxin by a laborious LC/MS−MS study recently carried out in our laboratories.[10] Such a study was focused on fully interpreting the highly articulate fragmentation pattern of palytoxin, with the ultimate purpose of deriving insights into the chemical structure of other still uncharacterized palytoxin-like compounds, by comparison of their MS−MS behavior with that of palytoxin itself.

As small as they may appear, the structural divergences between OVTX-a and palytoxin can crucially affect the toxicological profile of the former. By way of example, ostreocin-d, which shows small structural modifications in comparison to palytoxin, features almost the same mouse lethality as palytoxin, but a significantly reduced cytotoxicity and hemolytic potency.[11]

It follows that evaluation of OVTXs' toxicity constitutes a critical step in order to assess their real sanitary hazard. Eventually, the availability of pure OVTX-a, which is by far the main toxin produced by *O.* cf. *ovata*, heralds the potential of characterizing the risks it poses to humans as well as of establishing the tolerable daily intake for seafood consumers.

ASSOCIATED CONTENT

Supporting Information

NMR spectra (^{1}H−^{1}H COSY, z-filtered TOCSY, ROESY, HSQC, HSQCTOCSY, HMBC). Enlargements of NMR spectra crucial for assigning the chemical structure of ovatoxin-a. This material is available free of charge via the Internet at http://pubs.acs.org."

AUTHOR INFORMATION

Corresponding Author

forino@unina.it

ACKNOWLEDGMENTS

This work is a result of research supported by PRIN (Ministero dell'Istruzione, dell'Università e della Ricerca, 2009-Rome, Italy) and by ARPAC-Regione Campania, Italy (Piano di Monitoraggio Annuale per il Contenimento del Rischio Conseguente alla Fioritura di *Ostreopsis ovata* nelle acque costiere della Campania-Attività 2010).

REFERENCES

(1) Ciminiello, P.; Dell'Aversano, C.; Fattorusso, E.; Forino, M.; Magno, G. S.; Tartaglione, L.; Grillo, C.; Melchiorre, N. *Anal. Chem.* **2006**, *78*, 6153−6159.

(2) Ciminiello, P.; Dell'Aversano, C.; Fattorusso, E.; Forino, M.; Tartaglione, L.; Grillo, C.; Melchiorre, N. *J. Am. Soc. Mass Spectrom.* **2008**, *19*, 111−120.

(3) Ciminiello, P.; Dell'Aversano, C.; Dello Iacovo, E.; Fattorusso, E.; Forino, M.; Grauso, L.; Tartaglione, L.; Guerrini, F.; Pistocchi, R. *Rapid Commun. Mass Spectrom.* **2010**, *24*, 2735−2744.

(4) EFSA panel on contaminants in the food chain. *EFSA J.* **2009**, *7* (12), 1−38. 1393.

(5) Hoshaw, R. W.; Rosowski, J. R. *Handbook of Phycological Methods*; Cambridge University Press: New York, 1973; pp 53−67.

(6) Guillard, R. R. L. *Culture of Marine Invertebrates Animals*; Plenum Press: New York, 1975; pp 26−60.

(7) Guerrini, F.; Pezzolesi, L.; Feller, A.; Riccardi, M.; Ciminiello, P.; Dell'Aversano, C.; Tartaglione, L.; Dello Iacovo, E.; Fattorusso, E.; Forino, M.; Pistocchi, R. *Toxicon* **2010**, *55*, 211−220.

(8) Ciminiello, P.; Dell'Aversano, C.; Dello Iacovo, E.; Fattorusso, E.; Forino, M.; Grauso, L.; Tartaglione, L.; Florio, C.; Lorenzon, P.; De Bortoli, M.; Tubaro, A.; Poli, M.; Bignami, G. *Chem. Res. Toxicol.* **2009**, *22*, 1851−1859.

(9) Kan, Y.; Uemura, D.; Hirata, Y.; Ishiguro, M.; Iwashita, T. *Tetrahedron Lett.* **2001**, *42*, 3197−3202.
(10) Ciminiello, P.; Dell'Aversano, C.; Dello Iacovo, E.; Fattorusso, E.; Forino, M.; Grauso, L.; Tartaglione, L. *JASMS*, in press.
(11) Ukena, T.; Satake, M.; Usami, M.; Oshima, Y.; Naoki, H.; Fujita, T.; Kan, Y.; Yasumoto, T. *Biosci. Biotechnol. Biochem.* **2001**, *65*, 2585−2588.